JMEPEG (2006) 15:201-207
DOI: 10.1361/105994906X95887

1059-9495/$19.00

Effects of Ti- and Zr-Based Interlayer Coatings on Hot-Filament Chemical Vapor Deposition of Diamond on High-Speed Steel

R. Polini, F. Pighetti Mantini, M. Braic, M. Amar, W. Ahmed, H. Taylor, and M.J. Jackson

(Submitted November 4, 2005; in revised form December 27, 2005)

The prospect of obtaining good adhesion of diamond films onto steel substrates is highly exciting because the achievement of this objective will open up numerous new applications in industry. However, a major problem with depositing diamond onto steel is high diffusion of carbon into steel at chemical vapor deposition (CVD) temperatures leading to a very low nucleation density and cementite (Fe_3C) formation. Therefore, the study of the nucleation and growth processes is timely and will yield data that can be utilized to get a better understanding of how adhesion can be improved. This work focuses on the adhesion of thin diamond films onto high speed steel previously coated with various interlayers such as ZrN, ZrC, TiC, and TiC/Ti(C,N)/TiN. The role of seeding on nucleation density and the effect of diamond film thickness on stress development and adhesion has been investigated using scanning electron microscopy (SEM), x-ray diffraction (XRD), and Raman spectroscopy (RS). The main emphasis in this study lies with TiC, which for the first time proved to be a suitable layer for diamond CVD on high-speed steel (HSS). In fact, different from other interlayer materials investigated, no delamination was observed after 3 h of CVD at 650 °C when TiC was used. Nevertheless, the increase of diamond film thickness on TiC-coated HSS substrates led to delamination of small areas. This occurrence suggests that there was a distribution of adhesive toughness values at the diamond/TiC interface with the stress development being dependent on film thickness.

Keywords adhesion, CVD, diamond, interlayers, steel

1. Introduction

In recent years, a considerable amount of research has been done on coating/substrate systems where there is a large thermal mismatch between the coating and the substrate material (Ref 1, 2). As a consequence, during the heating and cooling stages of the deposition process large thermal stresses are induced causing the films to crack and delaminate from the substrate. To overcome these problems researchers have investigated several approaches to improve film adhesion and nucleation. These include the scratching of the substrate surface with abrasive powders, seeding with diamond crystals, substrate biasing, coating the substrate with thin films of metal or refractory compounds, ion implantation of substrate surfaces, and chemical etching of substrate surfaces (Ref 3). Steel substrates are of particular interest because they are widely used for the manufacture of a range of engineering components and tools, such as taps, dies, twist drills, reamers, saw blades, and other cutting tools.

Even though the properties of steel are well suited for most of the applications mentioned above, for more demanding applications the deposition of an adherent diamond coating by chemical vapor deposition (CVD) onto the steel can have significant advantages. The high hardness, high thermal conductivity, chemical inertness, and remarkable wear-resistant properties combine to make diamond one of the most promising coating materials available today (Ref 4). The combined properties of the diamond/steel system should yield properties much superior to those of steel and diamond individually allowing enhanced product performance and life.

However, direct diamond growth from the gas phase onto ferrous alloys is a serious problem, due mainly to the diffusion of carbon into steel at the high temperatures encountered during CVD. This leads to very low nucleation densities, cementite (Fe_3C) and graphite formation, and degradation of steel properties. In addition, the large difference in thermal expansion coefficients between steel and diamond induce high compressive stresses at the interface, causing film delamination. An elegant approach to this problem is to use interlayer materials that have thermal expansion coefficients with values between those of diamond and steel. This approach would decrease the effects of interfacial stresses, carbon diffusion, and sp^2 carbon formation at the interface during the CVD growth process. Although this approach has yielded partial success, residual stresses are still large enough to cause delamination. Singh et al. (Ref 5) reported a new approach to reduce interfacial stresses and to enhance bonding between diamond films and large thermal expansion coefficient mismatched substrates, such as stainless steel and Co-cemented tungsten carbide. They

This paper was presented at the fourth International Surface Engineering Congress and Exposition held August 1-3, 2005 in St. Paul, MN.

R. Polini and **F. Pighetti Mantini,** Dipartimento di Scienze e Tecnologie Chimiche, Università di Roma Tor Vergata, Via della Ricerca Scientifica, 00133 Rome, Italy; **M. Braic,** National Institute for Optoelectronics, Surface-Processing Laboratory, P.O. Box MG 05, Bucharest, Romania; **M. Amar, W. Ahmed,** and **H. Taylor,** Department of Chemistry and Materials, Manchester Metropolitan University, Chester Street, Manchester M1 5GD, U.K.; and **M.J. Jackson,** Birck Nanotechnology Center, Purdue University, West Lafayette, Indiana, IN 47907. Contact e-mail: jacksomj@purdue.edu.

used multiple nanosecond laser pulses with energies close to the abrasion threshold to create microrough structures at the substrate surfaces. This substrate pretreatment, followed by diamond CVD, led to the formation of a three-dimensional (3D) interface, which is expected to increase the adhesive strength by modifying the stress distribution in the diamond coating. On WC-Co substrates, Sein et al. (Ref 6, 7) used a chemical approach to roughen the surface and remove cobalt from the surface region. They showed that enhanced nucleation densities were achieved using a hot-filament chemical vapor deposition/bias-enhanced nucleation (HFCVD-BEN) growth stage after two-step chemical etching (Ref 7). Buijnsters et al. (Ref 8) reported the use of a 2.5 μm thick CrN interlayer for diamond deposition on steel at 650 °C. The formation of Cr carbide and the resulting microstructure played a role in enhancing the adhesion of diamond films. Borges et al. (Ref 9) used a nitriding process for increasing the amount of CrN on the surface of 304SS, which led to a more uniform diamond film. During the nitridation process, the Cr reaches the surface by diffusion resulting in the formation of mixed CrN and Cr_2N crystalline phases. Beside carbon nucleation, Cr carbides are also formed during diamond deposition, resulting in a layer mainly of carbides and carbon phases, and the continuous diamond films are grown on this layer. Glozman et al. (Ref 10) and Shang et al. (Ref 11) also reported the use of CrN interlayers as an effective method for growing diamond films on steel. On the other hand, the use of TiC as a barrier layer on steel has not been investigated in depth compared with other interlayers. To improve the adhesion of diamond on WC-Co tools Raghuveer et al. (Ref 12) used a TiN/TiC layer as a diffusion barrier to stop Co migration from the bulk of the substrate toward the diamond crystals through the grain boundaries. In addition to chemical etching and hydrogen plasma treatment to remove/reduce the Co from the surface, they reported growth of high-quality adherent diamond coatings on WC substrates through the use of this multilayer applied to steel. Carbon diffusion into the steel can be stopped, releasing interfacial stresses, and mechanically interlocking the diamond crystallites onto the carbide surface attainable. To overcome such problems as carbon diffusion, sp^2 carbon formation, and thermal expansion coefficient mismatch, interlayers based on ZrN, ZrC, TiC, and TiC/Ti(C,N)/TiN have been investigated in this study. The function of an interlayer is threefold: first, to create a barrier layer between carbon and metallic substrates; second, to reduce the mismatch between the thermal expansion coefficients of diamond and the substrate material; and third, to enhance the nucleation density (Ref 13). To further promote nucleation, and thus, adhesion of diamond onto interlayered steel samples, substrates were seeded with nanodiamond particles prior to CVD diamond growth. This treatment enhanced diamond nucleation either by implanting tiny diamond fragments into the substrate surface, onto which diamond can subsequently grow, or by creating suitable defects at the substrate surface that favor the heterogeneous nucleation of diamond from the gas phase (Ref 14, 15).

2. Experimental Procedures

M2-grade high-speed steel (HSS) samples (12 × 12 × 1 mm) were polished using emery paper in the range of 600 to 2400 grit. The samples were polished on a rotary table with a 9 kg backing weight using a back-and-forth motion to provide an even surface finish. A Mitutoyo Surftest analyzer (Aurora, IL) was used to obtain an average surface roughness value of 0.05 μm. The samples were then ultrasonically cleaned with acetone for 5 min. The following nitride and carbide films—ZrN, ZrC, TiC, and TiC/Ti(C,N)/TiN—were then deposited on the HSS samples by the reactive cathodic arc method. The films were all of 10 μm thickness and were deposited at 250 °C. The deposition system is shown in Fig. 1.

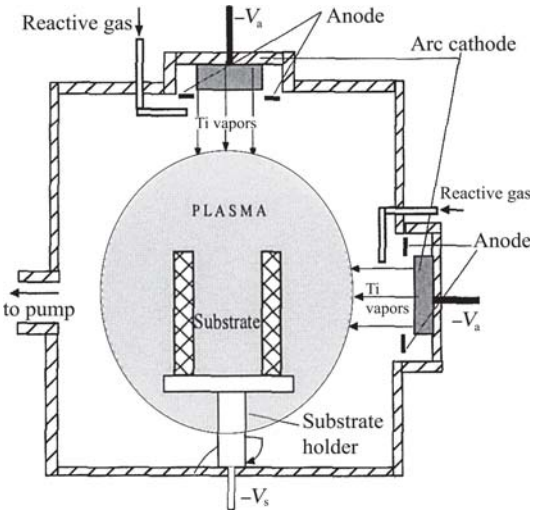

Fig. 1 Experimental PVD reactor

The system has two cathodic arc evaporators equipped with Ti and Zr targets, but for the work presented in this paper only one evaporator was used at a time. Nitride and carbide coatings were deposited only in N_2 and C_2H_2 atmospheres, respectively, while carbo-nitride coatings were obtained in a gas mixture of C_2H_2+N_2 whose composition was metered using mass flow controllers. The base pressure in the system was 5×10^{-4} Pa and the deposition pressure was maintained between 6×10^{-2} and 8×10^{-1} Pa. Preliminary experiments have shown that the highest microhardness values for the films were obtained for a substrate bias (V_s) of about −200 V and a cathodic arc current (I_a) of 90 A for Ti and 110 A for Zr. Before deposition, the samples were ultrasonically cleaned with trichloroethylene and mounted on a rotating holder inside the deposition chamber. Prior to deposition, the samples were sputtered using Ti or Zr ion bombardment (1 kV; 5 min). Before diamond deposition, the substrates were ultrasonically treated for 15 min with a 0.25 μm diamond powder suspension (DP-Suspension HQ, by Struers), followed by ultrasonic cleaning in acetone. The HFCVD system was built with a water-cooled stainless steel chamber as described previously (Ref 16). The gas sources were 1% methane in excess hydrogen. The pressure in the vacuum chamber was maintained at 4.8 kPa. The filament temperature was 2140 ± 30 °C, as measured using a two-color optical pyrometer (Land IR model RP 12). Substrate temperatures were between 620 and 650 °C and were monitored using a K-type thermocouple in direct contact with the sample. Under these experimental conditions, diamond growth rate was ~0.6 to 0.7 μm/h. After CVD, the sample was slowly cooled from the deposition temperature to room temperature in about 20 min. All physical vapor deposition (PVD) and CVD films were characterized by field emission scanning electron microscopy (FE-SEM, LEO Supra 35), and by x-ray diffraction (XRD, Philips X'Pert-Pro). XRD patterns (Cu Kα radiation, 40 kV, 40 mA) were acquired

using grazing incidence (1°) to analyze the films (interlayer and diamond) only. The quality of diamond films was assessed by Raman spectroscopy (Spex model Triple Mate). Raman spectra were collected using the 4880 Å radiation from an Ar^+ laser in the backscattered configuration.

3. Experimental Results and Discussion

3.1 Use of ZrN Interlayers

The possible problems with the cathodic arc deposition include stabilization and movement of the arc on the target surface. These result in the formation of molten micron-sized "globules" (or "macros") of the ejected material from the target surface (Ref 17). Figure 2 shows the SEM micrographs of ZrN coating deposited on HSS by reactive cathodic arc technique (panel a) and after 3 h of CVD (panel b). The morphology of the as-prepared ZrN coating showed a low surface density of macros with sizes not exceeding a few micrometers (Fig. 2a). After 3 h of CVD, the continuous diamond film underwent spontaneous delamination during cooling to room temperature (Fig. 2b). Figure 3 shows the XRD patterns of the as-deposited ZrN interlayer and after 3 h of CVD at slightly different temperatures (620 and 650 °C). The pattern of the interlayer before CVD showed peaks attributable to ZrN phase (JCPDS card No. 35-0753) (Ref 18) and very small amounts of metallic Zr (JCPDS card No. 05-0665) (Ref 19), probably embedded in ZrN globules. Further to diamond deposition, the ZrN peaks became sharper, due to the high CVD temperature that induced an increase of ZrN crystallite size. Moreover, after 3 h of CVD, XRD patterns showed the presence of diamond peaks, the disappearance of metallic Zr, and the formation of small amounts of monoclinic zirconia (ZrO_2, JCPDS card No. 37-1484) (Ref 20), confirmed in repeated CVD experiments using slightly different deposition temperatures. No ZrC peaks (JCPDS card No. 35-0784) (Ref 21) were detectable in the diffraction patterns after CVD. Therefore, zirconia formation during CVD occurred by oxidation of Zr in the CVD reactor. In fact, the gas phase in the reactor, which was not prebaked prior to CVD, should contain residual water molecules desorbing from the chamber walls, and this very low amount of H_2O (as well as its reaction products with atomic hydrogen, namely, OH radicals) could have been responsible for the oxidation of Zr. This fact indicates that Zr preferred to transform into ZrO_2 rather than ZrC under the HFCVD process conditions used.

3.2 Use of ZrC Interlayers

Figure 4 shows the SEM micrographs of ZrC film as deposited on HSS before diamond deposition (panel a) and after 3 h of CVD (panels b and c). After arc deposition, the ZrC coating showed a low surface density of macros (Fig. 4a). After 3 h of deposition, the diamond film underwent spontaneous delamination and only a few small areas remained covered with diamond film (Fig. 4b). The film in these areas was continuous (Fig. 4c), thus confirming the effectiveness of seeding in promoting nucleation densities as large as those required to obtain a continuous diamond film after 3 h of deposition. Figure 5 displays the XRD diffraction patterns of ZrC coatings before and after diamond deposition. In the diffraction pattern before deposition, only ZrC peaks (JCPDS card No. 35-0784) (Ref 21) were present. After 3 h of CVD, the peaks of ZrC became slightly sharper and a low-intensity diamond (111) peak was also detectable.

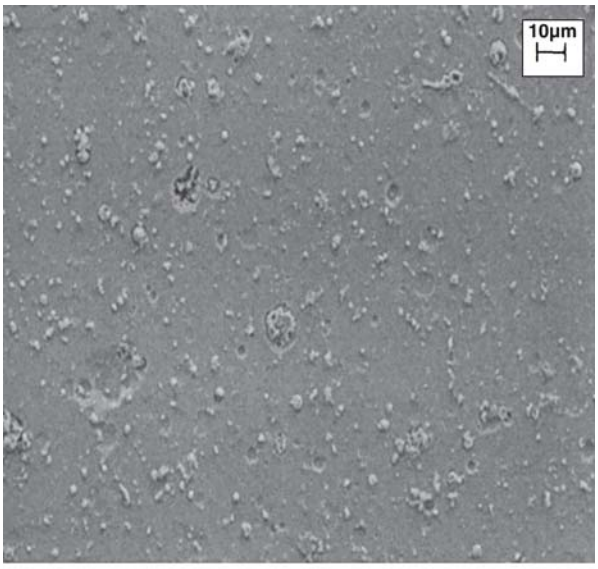

(a)

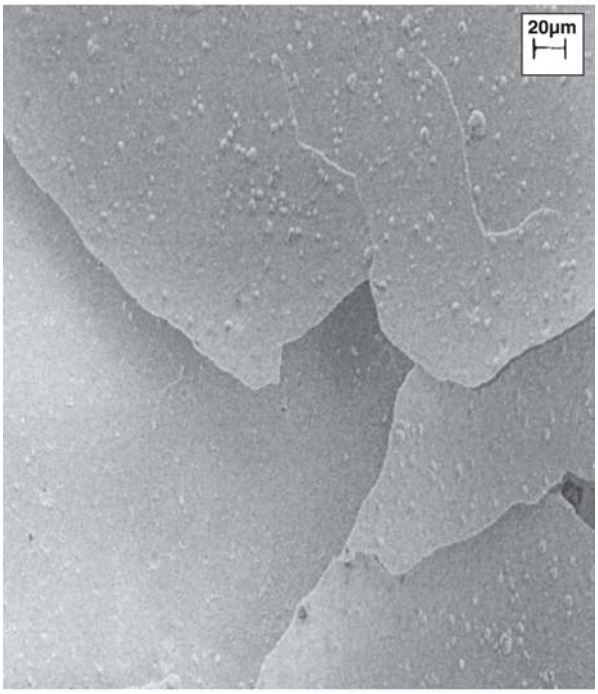

(b)

Fig. 2 Surface morphology of (a) ZrN interlayer on HSS samples and (b) diamond film remaining at the substrate surface after spontaneous delamination (T_{CVD} = 650 °C)

3.3 Use of TiC/Ti(C,N)/TiN Interlayers

Figure 6 shows the SEM micrographs of the films prepared using the experimental procedure as described earlier (panel a) and of the surface morphology after 3 h of CVD (panel b). The interlayer surface exhibited a low density of micrometer-sized macros (Fig. 6a). After 3 h of CVD, as observed in the previous cases, diamond film underwent spontaneous delamination (Fig. 6b), indicating that this layer was not effective as far as diamond deposition on HSS is concerned. Again, the diamond film in the remaining areas at the substrate surface was continuous. Figure 7 shows diffraction patterns of the multilayer

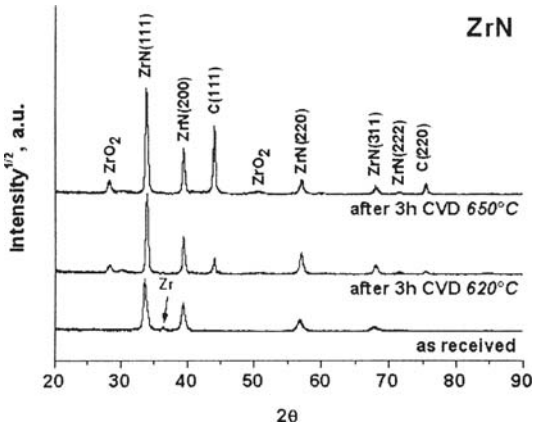

Fig. 3 XRD patterns of ZrN interlayers before and after 3 h of CVD

films before and after 3 h of CVD. The XRD pattern of the PVD coating showed the presence of peaks attributable to NaCl-type TiN phase (JCPDS card No. 38-1420) (Ref 22), a very low intensity Ti(101) peak, and an unknown peak at $2\theta = 32.86°$. Similar to other interlayers, after 3 h of deposition, the peaks of TiN became sharper. Moreover, diamond peaks were detectable, while both the Ti and unknown phase peaks disappeared. No TiC peaks were clearly visible after CVD. This fact suggests that Ti reacted with carbon and TiN during CVD to give rise to a small amount of TiC_xN_{1-x}, with $x \ll 1$, and therefore, with a lattice parameter close to that of TiN. Different from the case of ZrN interlayer, where metallic Zr was oxidized to ZrO_2 after 3 h of CVD, no titania formation was detected after diamond deposition. This fact can be explained by assuming that, under these experimental conditions, the reaction of Ti with carbon species represented a preferred reaction pathway rather than metal oxidation.

3.4 Use of TiC Interlayers

Figure 8 shows the SEM micrograph of TiC coating deposited on HSS by the reactive cathodic arc technique. The formation of macros is particularly critical in the reactive evaporation of TiC films. In fact, as shown in Fig. 8, a large density of macros, even larger than 10 μm, was present on the surface of TiC coatings prepared by conventional cathodic arc deposition. After 3 h of diamond deposition on TiC interlayered HSS, an adherent polycrystalline diamond film was obtained (Fig. 9). In fact, no delamination occurred after cooling down to room temperature. Following this encouraging and quite new result, further investigation of the role of diamond thickness on adhesion was performed. Therefore, it was decided to deposit another sample using double the deposition time (6 h). After 6 h of CVD, the diamond film underwent delamination in a few small areas, as shown in Fig. 10.

XRD patterns of TiC interlayers before and after 3 and 6 h of CVD are shown in Fig. 11. The XRD pattern of the as-evaporated TiC film showed broad peaks attributable to TiC phase (JCPDS card No. 32-1383) (Ref 23) and lower intensity Ti (101) and (002) peaks. After 3 h of CVD, the metallic Ti peaks disappeared, TiC peaks became sharper, and no other Ti-containing phases were detectable, thus indicating that both the carburization of Ti and the increase of TiC crystallite size occurred during diamond deposition. Both the full width at half maximum (FWHM) and the position of the TiC peaks after 3

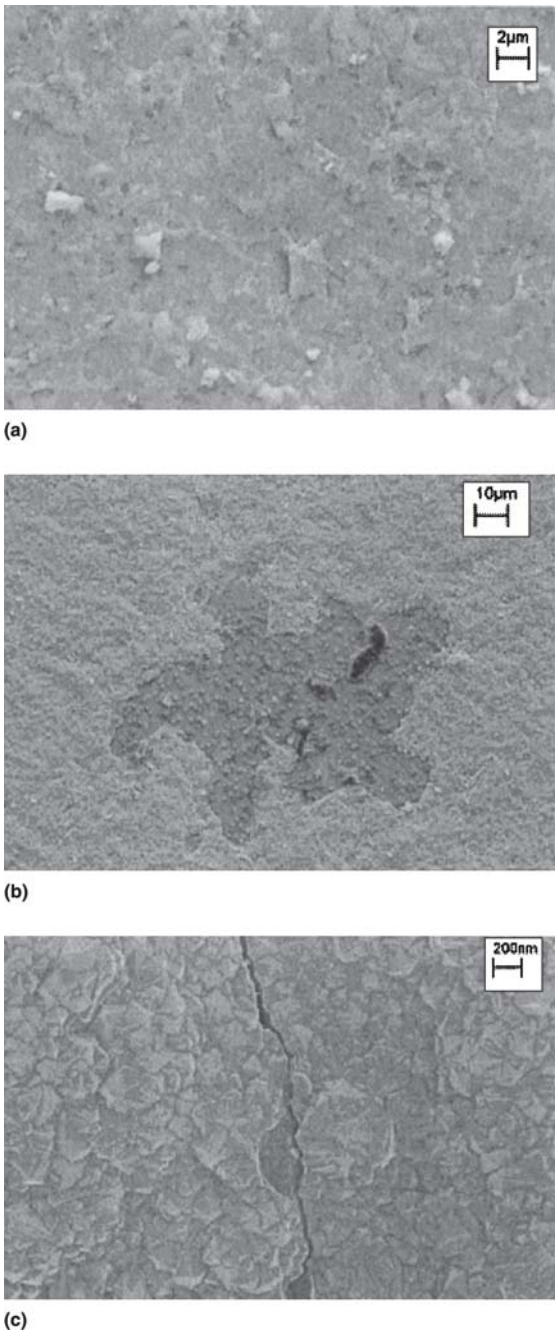

Fig. 4 Surface morphology of HSS samples with ZrC interlayer: (a) as deposited ZrC film; (b) substrate surface after 3 h of diamond CVD; (c) morphology of the diamond film remaining at the substrate surface after spontaneous delamination

and 6 h of CVD were the same. The only difference between the two diffraction patterns was the intensity of diamond peaks. Figure 12 displays the Raman spectra of the diamond films deposited for 3 and 6 h onto TiC interlayers. Both spectra showed a broad diamond signature centered at around 1345/cm and the initial splitting of the zero-phonon diamond peak. These findings are in agreement with the results of Buijnsters et al. (Ref 8), who studied the deposition of diamond on HSS using arc-plated Cr nitride interlayers.

The diamond for films deposited for 6 h was somewhat broader and shifted slightly toward larger wavenumbers, thus

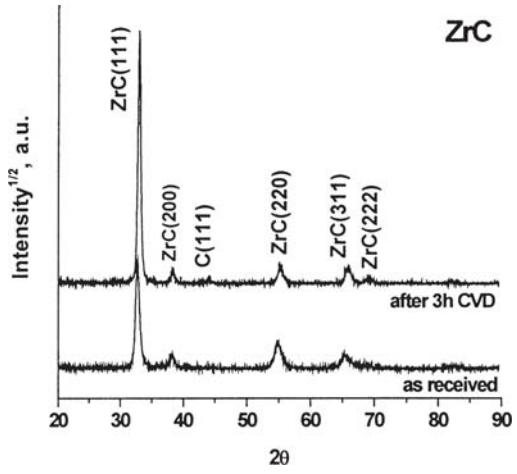

Fig. 5 XRD patterns of ZrC interlayers before and after 3 h of CVD

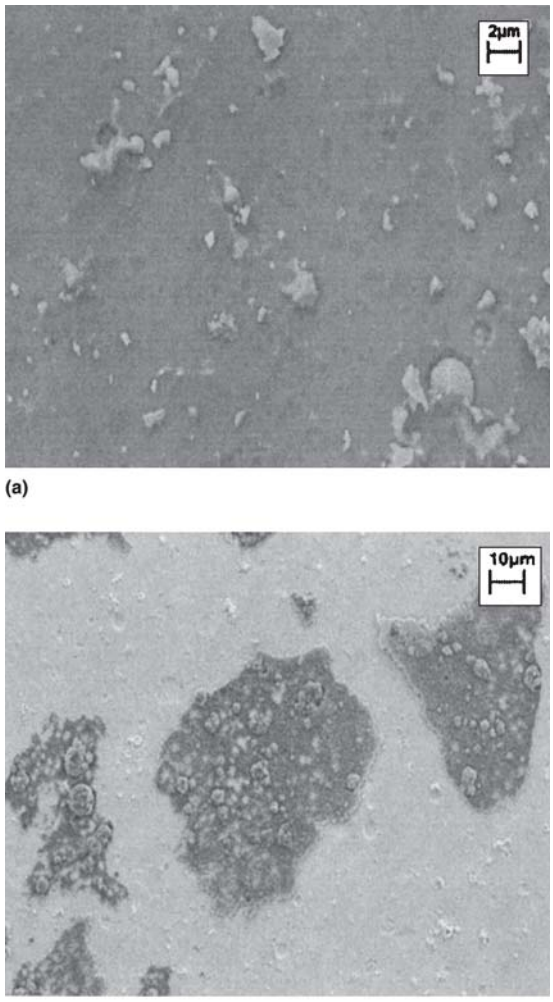

Fig. 6 Surface morphology of (a) TiC/Ti(C,N)/TiN multilayer on HSS samples and (b) diamond-coated areas remaining at the substrate surface after spontaneous delamination (T_{CVD} = 650 °C)

indicating a possible wider stress distribution, which developed with increasing film thickness. The fact that the diamond film after 6 h of deposition exhibited both a broad Raman peak and

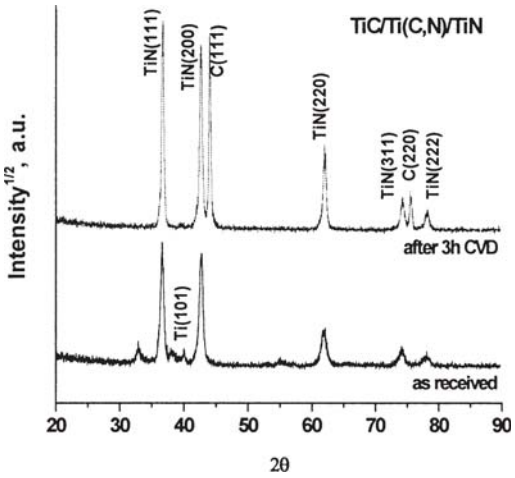

Fig. 7 XRD patterns of TiC/Ti(C,N)/TiN multilayer before and after 3 h of diamond CVD

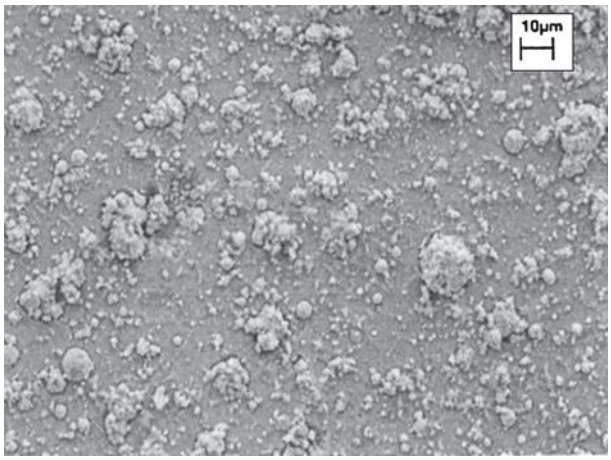

Fig. 8 SEM micrograph of the TiC coating deposited on HSS by cathodic arc deposition

a huge shift was a clear indication that diamond remaining at the substrate surface was still adherent. This suggests that there was a population of adhesive toughness values at the diamond/TiC interface. The diamond delaminated in correspondence to those areas where the adhesion was lower and the interfacial stresses exceeded, due to increased film thickness and the adhesive strength of the diamond/TiC system. The distribution of adhesive toughness values and/or stresses can be attributed to the morphology of the 3D interface between diamond and the very rough TiC interlayer, as predicted by Singh and coworkers (Ref 5).

4. Conclusions

Zr- and Ti-based PVD coatings were deposited at 250 °C on M2-grade HSS to investigate their potential use as interlayers for diamond CVD. The high CVD temperature induced minor changes in the interlayers, namely the increase of crystallite size. Small amounts of Zr were present in evaporated ZrN interlayers, as well as small quantities of Ti were detected in Ti-based interlayers. After 3 h of diamond deposition, these

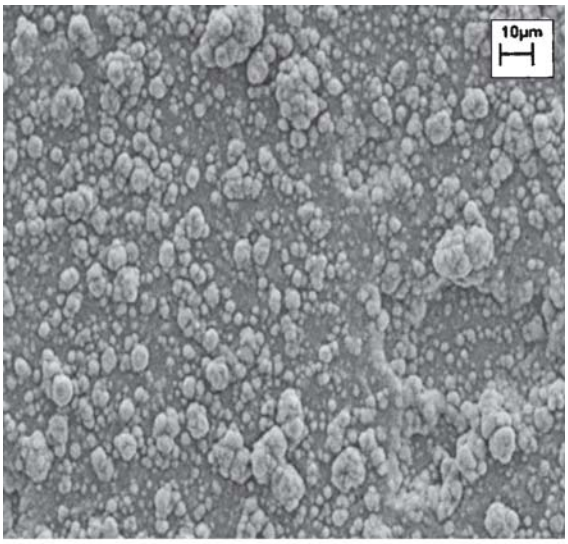

(a)

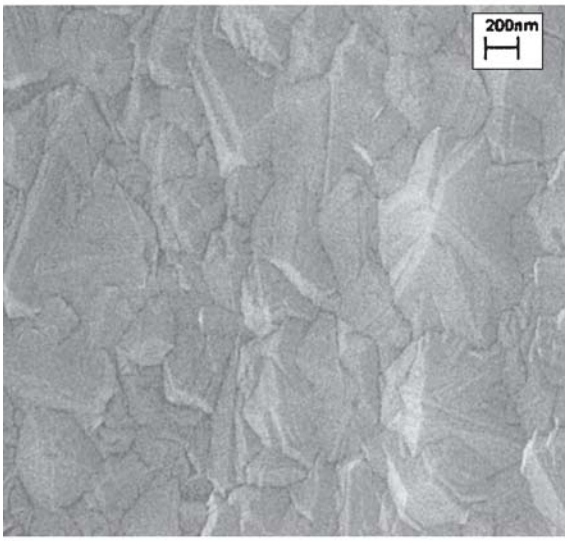

(b)

Fig. 9 SEM micrographs showing the adherent diamond film grown after 3 h of CVD on TiC interlayered HSS: (a) surface morphology of the diamond/TiC coating, (b) microstructure of the diamond film

metallic phases disappeared. Only metallic Zr in ZrN interlayer preferentially reacted with traces of water vapor and/or OH radicals inside the CVD chamber to form monoclinic zirconia. The overall results indicate that TiC was the sole interlayer, among those investigated, suitable for deposition of thin diamond films on HSS. In fact, the continuous diamond film formed after 3 h of CVD on TiC interlayered HSS did not undergo any spontaneous delamination after cooling the substrate from the deposition temperature to room temperature. To the best of our knowledge, this is the first time that arc-deposited TiC interlayers have been effective for the growth of adherent diamond on tool steels. Nevertheless, the increase of diamond film thickness on TiC-coated steel substrates led to delamination of small diamond areas. This suggests that there is a distribution of adhesive toughness values at the diamond/TiC interface with the stress development being dependent on film thickness. It is still debatable whether the adhesion of diamond films is entirely due to the pronounced 3D interface

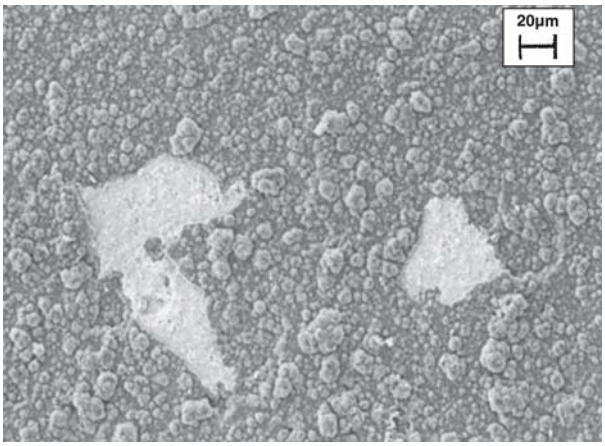

Fig. 10 SEM micrograph showing small areas where delamination of the diamond film on TiC interlayered HSS occurred after 6 h of CVD

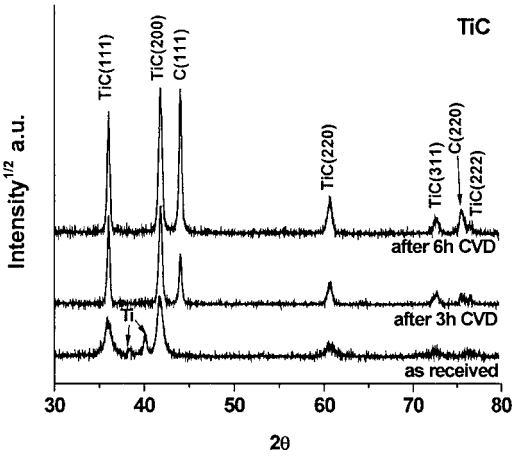

Fig. 11 XRD patterns of TiC interlayers before and after 3 and 6 h of CVD

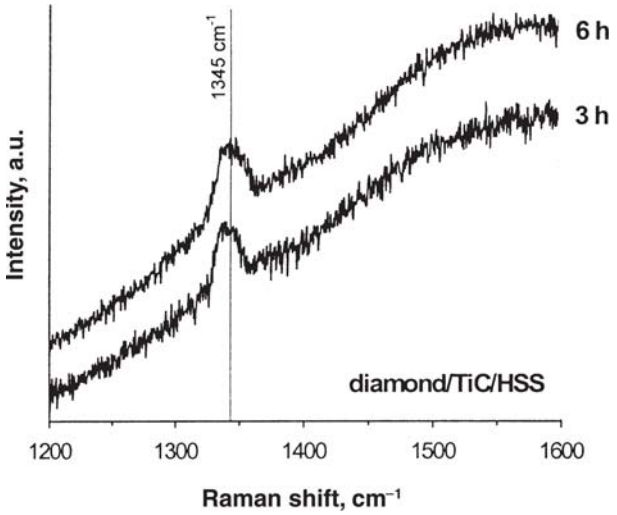

Fig. 12 Raman spectra of diamond films deposited for 3 and 6 h on TiC interlayered HSS

between diamond and TiC or to this coating creating stronger chemical bonds with sp^3 carbon. More work is required to comprehend the fundamental aspects of adhesion of diamond films onto TiC-interlayered steel.

References

1. I. Endler, A. Leonhardt, H. Scheibe, and R. Born, Interlayers for Diamond Deposition on Tool Materials, *Diamond Relat. Mater.,* 1996, **5,** p 299-303
2. A. Silva, A.P.M. Baptista, E. Pereira, Q.H. Fan, A.J.S. Fernandes, and F.M. Costa, Microwave Plasma CVD Diamond Nucleation on Ferrous Substrates with Ti and Cr Interlayers, *Diamond Relat. Mater.,* 2002, **11,** p 1617-1622
3. M. Nesládek, K. Vandierendonck, C. Quaeyhaegens, M. Kerkhofs, and L.M. Stals, Adhesion of Diamond Coatings on Cemented Carbides, *Thin Solid Films,* 1995, **270,** p 184-188
4. C. Chang, Y. Liao, G.Z. Wang, Y.R. Ma, and R.C. Fang, *CVD Diamond Growth, Crystal Growth Technology*, B. Byrappa, Ed., Noyes Publications, Westwood, NJ, 2003, p 396-400
5. R. Singh, D. Gilbert, J. Fitzgerald, S. Harkness, and D. Lee, New Diamond and Frontier Carbon Technology, *Science,* 1996, **272,** p 396-400
6. H. Sein, W. Ahmed, M.J. Jackson, R. Woodward, and R. Polini, Performance and Characterization of CVD Diamond Coated, Sintered Diamond, and WC-Co Tools for Dental and Micromachining Applications, *Thin Solid Films,* 2004, **447-448,** p 455-461
7. H. Sein, W. Ahmed, M. Jackson, R. Polini, I. Hassan, M. Amar, and C. Rego, Enhancing Nucleation Density and Adhesion of PCD Films Deposited by HFCVD Using Surface Treatments on Co-Cemented WC, *Diamond Relat. Mater.,* 2004, **13,** p 610-615
8. J.G. Buijnsters, P. Shankar, W. Fleischer, W.J.P. Van Enckevort, J.J. Schermer, and J.J. Meulen, CVD Diamond Deposition on Steel Using Arc Plated CrN Interlayers, *Diamond Relat. Mater.,* 2002, **11,** p 536-544
9. C. Borges, E. Pfender, and J. Heberlein, Influence of Nitrided and Carbonitrided Interlayers on Enhancement of Diamond on 304 Stainless Steel, *Diamond Relat. Mater.,* 2001, **10,** p 1983-1990
10. O. Glozman, G. Halperin, I. Etsion, A. Berner, D. Shectman, G. Lee, and A. Hoffman, Study of the Wear Behavior of Diamond Films Deposited on Steel Substrates by Using CrN Interlayer, *Diamond Relat. Mater.,* 1999, **8,** p 859-864
11. N. Shang, Z. Zhou, C. Lee, I. Bello, and S. Lee, Effect of Ion Beam Nitriding on Diamond Nucleation and Growth on Steel Substrates, *Diamond Relat. Mater.,* 2001, **10,** p 1506-1510
12. M. Raghuveer, S. Yoganand, K. Jagannadham, R. Lemaster, and J. Bailey, Improved CVD Diamond Coatings on WC-Co Tool Substrates, *Wear,* 2002, **253,** p 1194-1206
13. Q. Fan, A. Fernandes, and J. Gracio, Diamond Coatings on Steel with a Ti-Interlayer, *Diamond Relat. Mater.,* 1998, **7,** p 603-606
14. S. Iijima, Y. Aikawa, and K. Baba, CVD of Diamond on Various Substrates, *J. Mater. Res.,* 1991, **6,** p 1491-1503
15. E. Molinari, R. Polini, and M. Tomellini, Diamond Crystallite Formation on Si (110) from the Gas Phase: Seeding or Heterogeneous Nucleation, *Appl. Phys. Lett.,* 1992, **61,** p 1287-1289
16. R. Polini, G. Marcheselli, and E. Traversa, Deposition of Diamond on WC Ceramic Materials Using HFCVD, *J. Am. Ceram. Soc.,* 1994, **77,** p 2043-2048
17. R.F. Bunshah, Ed., *Handbook of Deposition Technologies for Films and Coatings,* 2nd ed., Noyes Publications, Westwood, NJ, 1994, p 164
18. JCPDS 35-0735, International Center for Powder Diffraction Data, Swarthmore, PA, 1989
19. JCPDS 05-0665, International Center for Powder Diffraction Data, Swarthmore, PA, 1989
20. JCPDS 37-1484, International Center for Powder Diffraction Data, Swarthmore, PA, 1989
21. JCPDS 05-0784, International Center for Powder Diffraction Data, Swarthmore, PA, 1989
22. JCPDS 38-1420, International Center for Powder Diffraction Data, Swarthmore, PA, 1989
23. JCPDS 32-1383, International Center for Powder Diffraction Data, Swarthmore, PA, 1989